Available online at www.sciencedirect.com

ScienceDirect

Advances in Space Research 57 (2016) 1641–1651

ADVANCES IN SPACE RESEARCH (a COSPAR publication)

www.elsevier.com/locate/asr

Hybrid perturbation methods based on statistical time series models

Juan Félix San-Juan [a,*], Montserrat San-Martín [a], Iván Pérez [a], Rosario López [b]

[a] Scientific Computing Group (GRUCACI), University of La Rioja, 26004 Logroño, Spain
[b] Scientific Computing Group (GRUCACI), Center for Biomedical Research of La Rioja (CIBIR), 26006 Logroño, Spain

Received 30 October 2014; received in revised form 9 May 2015; accepted 16 May 2015
Available online 22 May 2015

Abstract

In this work we present a new methodology for orbit propagation, the hybrid perturbation theory, based on the combination of an integration method and a prediction technique. The former, which can be a numerical, analytical or semianalytical theory, generates an initial approximation that contains some inaccuracies derived from the fact that, in order to simplify the expressions and subsequent computations, not all the involved forces are taken into account and only low-order terms are considered, not to mention the fact that mathematical models of perturbations not always reproduce physical phenomena with absolute precision. The prediction technique, which can be based on either statistical time series models or computational intelligence methods, is aimed at modelling and reproducing missing dynamics in the previously integrated approximation. This combination results in the precision improvement of conventional numerical, analytical and semianalytical theories for determining the position and velocity of any artificial satellite or space debris object. In order to validate this methodology, we present a family of three hybrid orbit propagators formed by the combination of three different orders of approximation of an analytical theory and a statistical time series model, and analyse their capability to process the effect produced by the flattening of the Earth. The three considered analytical components are the integration of the Kepler problem, a first-order and a second-order analytical theories, whereas the prediction technique is the same in the three cases, namely an additive Holt–Winters method.
© 2015 COSPAR. Published by Elsevier Ltd. All rights reserved.

Keywords: Artificial satellite theory; Orbit propagator; Hybrid perturbation method; Time series

1. Introduction

The equations of the perturbed motion of a satellite can be written as a set of 3 second-order or 6 first-order ordinary differential equations. The orbit propagation problem consists in computing the position and velocity of the satellite at a given final time t_f, from the position and velocity at a given initial time t_1. Classically, the techniques used to solve this problem have been three.

The first two methods are known as general and special perturbation techniques. General perturbation techniques are based on the analytical integration of the satellite's equations of motion using perturbation theories (Deprit, 1969; Giacaglia, 1964; Hori, 1966, 1971; Krylov and Bogoliubov, 1947; Morrison, 1965). These techniques provide approximate analytical solutions (Aksnes, 1970; Brouwer, 1959; Hoots and Roehrich, 1980; Hoots and France, 1987; Kinoshita, 1977; Kozai, 1962; Lyddane, 1963) valid for any set of initial conditions. These solutions are explicit functions of time, physical parameters and integration constants, which are mainly characterised by retaining the essential behaviour of the motion. It is worth noting that most analytical theories currently in use only consider very basic models of external forces, because in

* Corresponding author. Tel.: +34 941299440; fax: +34 941299460.
E-mail addresses: juanfelix.sanjuan@unirioja.es (J.F. San-Juan), montse.sanmartin@unirioja.es (M. San-Martín), ivan.perez@unirioja.es (I. Pérez), rlgomez@riojasalud.es (R. López).

http://dx.doi.org/10.1016/j.asr.2015.05.025
0273-1177/© 2015 COSPAR. Published by Elsevier Ltd. All rights reserved.

some cases their corresponding analytical expressions can be too cumbersome. Furthermore, only low-order approximations are taken into account because analytical expansions for the higher-order solutions may become unmanageably long. Some of these theories can even implement truncated dynamic parameter expansions, so that their accuracy and computational efficiency are closely related to the initial assumptions.

On the other hand, special perturbation methods (Berry and Healy, 2004; Kinoshita and Nakai, 1989; Long et al., 1989) refer to the accurate numerical integration of the equations of motion, including any external forces, even those in which analytical manipulations are complicated, which makes it necessary to use small steps in order to integrate the equations of motion. General perturbation methods produce more computationally efficient propagators although are not as accurate as those developed using special perturbation techniques.

Finally, the third approach is the semianalytical technique (Cefola et al., 2009; Liu and Alford, 1980; Neelon et al., 1997), which combines and takes advantage of the best characteristics of both the general and special perturbation techniques. This approach allows to include any external forces in the equations of motion, which are simplified using analytical techniques. Thus, the transformed equations of motion can be integrated numerically in a more efficient way by using longer integration steps.

Current needs for Space Situational Awareness require improving orbit propagation of space objects in different ways, including the efficient short-term propagation of catalogues of thousands of objects, the accurate very-long-term propagation needed for designing disposal strategies, the instant propagation of fragmentation models, or the propagation of uncertainties in observed orbits of *potentially hazardous objects*, among others.

Improvement in the models to be integrated constitutes a basic line of research, together with the use of advanced computer architectures based on parallel processing. Additional improvement can be achieved by combining both integrating and forecasting techniques, which we have called hybrid methods.

In this work we present the hybrid perturbation theory, which may combine any kind of the aforementioned integration techniques with forecasting techniques based on statistical time series models (Chan, 2010; Trapletti and Hornik, 2011; San-Juan et al., 2012) or computational intelligence methods (Pérez et al., 2013). This combination allows for an increase in the accuracy of the numerical, analytical or semianalytical theories for predicting the position and velocity of any artificial satellite or space debris object, through the modelling of higher-order terms and other external forces not considered in those initial theories, as well as some physical effects not accurately modelled by the mathematical equations. The final goal of hybrid methodology is to complement the mathematical model of an orbiter dynamics, which is never a completely faithful representation of physical phenomena, with real dynamics provided by real observations, thus yielding a more accurate representation of real behaviour. As a first step in the process to eventually include unmodelled physical effects in the formulation of the problem, we start by considering a basic perturbation, J_2, and check the capability of the hybrid propagator to grasp its dynamics. In this process we simulate real observations by means of numerically generated ephemeris through an 8th order Runge–Kutta method (Dormand and Prince, 1989).

The aim of this paper is to develop a family of hybrid orbit propagators based on three different orders of approximation of an analytical theory, in order to model the effect produced by the flattening of the Earth so that this technique can be validated. These hybrid orbit propagators incorporate the integration of the Kepler problem in the first case, a first-order analytical theory in the second case and a second-order analytical theory in the last case as the integration techniques; the forecasting technique is an additive Holt–Winters method in the three cases.

This paper is organised as follows. Section 2 describes the concept that underlies hybrid perturbation methodology. Section 3 outlines the second-order analytical theory PPD that, together with its first-order and zero-order approximations, constitutes the base for the three hybrid propagators to be developed in the following sections. Section 4 describes the Holt–Winters method, an exponential smoothing technique used in this paper as the forecasting part of the hybrid propagators. In Section 5, the construction of the three hybrid propagators is detailed, paying special attention to the preliminary statistical analysis of control data, which is important in order to choose the most appropriate sampling rate for the time series to be processed. Results are analysed, and compared to the conventional analytical propagation results, for a set of 9 LEO satellites. Finally, Section 6 summarises the study and remarks some interesting findings.

2. Hybrid perturbation methodology

A hybrid perturbation theory is a methodology for determining an estimation of the position and velocity of any orbiter, which may be an artificial satellite or space debris object, at a final instant t_f, in some set of canonical or non-canonical variables, $\hat{\boldsymbol{x}}_{t_f}$.

In a first phase, an integration method $\mathcal{I}$ is needed in order to calculate a first approximation, $\boldsymbol{x}^{\mathcal{I}}_{t_f}$, from the position and velocity at an initial instant $t_1, \boldsymbol{x}_{t_1}$:

$$\boldsymbol{x}^{\mathcal{I}}_{t_f} = \mathcal{I}(t_f, \boldsymbol{x}_{t_1}). \tag{1}$$

This approximation can include some inaccuracies derived from the facts that, for the sake of manageability of the resulting expressions and affordability of the subsequent computations, not all the external forces are usually taken into account in the physical model, and only low-order approximations are considered. Additional

imprecision arises from the fact that mathematical models of perturbations not always depict real physical phenomena with high fidelity.

The error of this approximation for any instant $t_i, \boldsymbol{\varepsilon}_{t_i}$, can be determined if the exact position and velocity $\boldsymbol{x}_{t_i}$ is known, usually through a precise observation:

$$\boldsymbol{\varepsilon}_{t_i} = \boldsymbol{x}_{t_i} - \boldsymbol{x}^{\mathcal{I}}_{t_i}. \tag{2}$$

The second phase of the method requires the knowledge of $\boldsymbol{x}_{t_i}$ for $t_1, \ldots, t_T$, with $t_T < t_f$, in order to build the time series of errors $\boldsymbol{\varepsilon}_{t_1} \ldots \boldsymbol{\varepsilon}_{t_T}$ that contains the dynamics not present in the approximation generated during the first phase. The time elapsed between t_1 and t_T is defined as control period, $\boldsymbol{\varepsilon}_{t_1} \ldots \boldsymbol{\varepsilon}_{t_T}$ as control data and T as the number of points in the control period. Then the goal is the modelling of such dynamics in order to be able to reproduce it; this task is accomplished by means of statistical techniques in time series analysis or computational intelligence methods. Once it has been done, an estimation of the error at the final instant $t_f, \hat{\boldsymbol{\varepsilon}}_{t_f}$, can be calculated, and consequently the desired value of $\hat{\boldsymbol{x}}_{t_f}$ can be determined as:

$$\hat{\boldsymbol{x}}_{t_f} = \boldsymbol{x}^{\mathcal{I}}_{t_f} + \hat{\boldsymbol{\varepsilon}}_{t_f}. \tag{3}$$

It is worth noting that this methodology can be applied to any kind of integration methods regardless of the fact that in this work it has been applied to an analytical theory. For this case, Fig. 1 shows the instants at which both the analytical expression and the statistical time series model have to be evaluated.

3. Second-order analytical theory PPD

The *main problem* of the artificial satellite theory is defined as a Kepler problem perturbed by Earth's oblateness. This model provides a first approximation to describe the motion of a low Earth orbiter. In this Section we develop a second-order closed-form analytical theory, based on Lie transforms, for the main problem, which we will use to derive the analytical part of the three hybrid orbit propagators to be analysed in Section 5. In the first case, a zero-order approximation, i.e. the Kepler solution, will be considered, whereas a first-order and the complete second-order approximations will be taken into account for the remaining two cases.

The main-problem dynamical system can be described in a cartesian coordinate system $(\boldsymbol{x}, \boldsymbol{X})$ by means of the Hamiltonian

$$\mathcal{H} = \frac{1}{2}(\boldsymbol{X} \cdot \boldsymbol{X}) - \frac{\mu}{r}\left[1 - J_2\left(\frac{\alpha}{r}\right)^2 P_2\left(\frac{z}{r}\right)\right], \tag{4}$$

where $r = \sqrt{x^2 + y^2 + z^2}$ is the geocentric distance, P_2 represents the Legendre polynomial of degree 2, μ is the gravitational constant, α is the equatorial radius of the Earth, and $J_2 > 0$ is a constant representing the shape of the Earth.

In order to carry out a second-order analytical theory, the Hamiltonian (4) is rewritten in terms of Delaunay variables (l, g, h, L, G, H). This set of canonical action-angle variables can be directly related to the orbital elements through the following expressions:

$$\begin{aligned} l &= M, \quad & L &= \sqrt{\mu a}, \\ g &= \omega, \quad & G &= \sqrt{\mu a(1-e^2)}, \\ h &= \Omega, \quad & H &= \sqrt{\mu a(1-e^2)}\cos i, \end{aligned} \tag{5}$$

where M is the mean anomaly, ω the argument of the perigee, Ω the longitude of the ascending node, a the semi-major axis, e the eccentricity and i the inclination. Therefore, the transformed Hamiltonian in Delaunay variables yields

$$\mathcal{H} = -\frac{\mu^2}{2L^2} - \frac{\epsilon}{2}\frac{\mu}{r}\left(\frac{\alpha}{r}\right)^2 (1 - 3s^2 \sin^2(f+g)), \tag{6}$$

where $\epsilon = J_2$ is a small parameter, $s = \sin i$ and f is the true anomaly.

Next, following the method described in Deprit (1969), three Lie transforms are applied in order to remove the long-period terms due to the argument of the perigee in the first place (Alfriend and Coffey, 1984; Deprit, 1981), and then the short-period terms due to the mean anomaly (Deprit, 1982). Finally, the transformed Hamiltonian yields, up to second order,

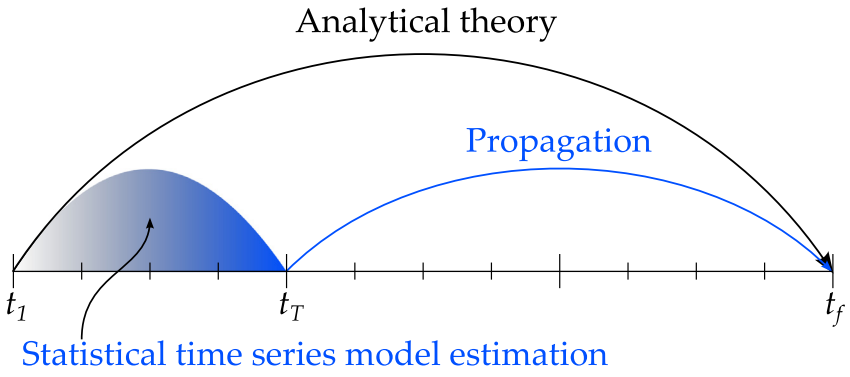

Fig. 1. Evaluation of a hybrid propagator based on the combination of an analytical theory and a statistical time series model.

$$\mathcal{K} = -\frac{\mu^2}{2L''^2} + \epsilon\frac{\alpha^2\mu^4}{4\eta''^3 L''^6}(3s''^2 - 2) - \epsilon^2\frac{3\alpha^4\mu^6}{128\eta''^7 L''^{10}}\left[(5\eta''^2 + 36\eta'' + 35)s''^4 + 8(\eta''^2 - 6\eta'' - 10)s''^2 - 8(\eta''^2 - 2\eta'' - 5)\right], \quad (7)$$

where $\eta'' = \sqrt{1 - e''^2}$. It is worth noting that $\mathcal{K}$ is independent of the variables l'', g'' and h'', and thus Hamilton's equations can be easily integrated by quadratures.

The algebraic manipulations required to develop this analytical theory and its corresponding analytical orbit propagator program were built using a set of *Mathematica* packages called MathATESAT (San-Juan et al., 2011), which is a reimplementation of the ATESAT (San-Juan, 1994, 1998). The acronym PPD makes reference to the sequence of Lie transforms used to carry out this analytical theory; in this case, the involved transforms are the elimination of the Parallax, the elimination of the Perigee and the Delaunay normalisation.

4. Time series forecasting using exponential smoothing methods

Exponential smoothing methods are forecasting algorithms for time series. Their main advantages are their ease of application, speed and reduced computational burden. Predictions generated by these methods are based on previously collected data, giving higher importance to more-recent observations. These methods assume a time series is the combination of three components: the trend or long-term variation, the seasonal component, which represents periodic oscillations that repeat at constant intervals, and the irregular or non-predictable component. There are two main procedures for combining these components, depending on the cyclic behaviour with respect to the trend: the additive and the multiplicative compositions. In the additive case, the series shows stable cyclic fluctuations, independently of the increase in the series level. On the contrary, the multiplicative model implies a change in the amplitude of the seasonal oscillations as the series trend varies. It is worth noting that a multiplicative model can be converted into an additive one through a Box-Cox transformation.

In mathematical terms, a time series, ε_t, can be decomposed into trend, μ_t, seasonal variation, s_t, and irregular or non-predictable component, v_t. In an additive model, these components combine in the following manner:

$$\varepsilon_t = \mu_t + s_t + v_t. \quad (8)$$

In particular, the Holt–Winters method (Winters, 1960) combines a linear trend together with a periodic behaviour. In this method, the trend can be expressed as:

$$\mu_t = a + bt, \quad (9)$$

where a and b represent the level and slope of the series, respectively.

This method predicts the series value at time t according to the following recursive procedure

$$\hat{\varepsilon}_t = A_{t-1} + B_{t-1} + S_{t-s}, \quad (10)$$

that is, the addition of level, A_{t-1}, and slope, B_{t-1}, at the previous instant, plus seasonal variation, S_{t-s}, s epochs before, thus being s the period of such seasonal variation.

The corresponding algorithm updates, at every epoch, the level, the slope of the trend and the values of the seasonal factors, by means of three equations. The first equation determines the series level at epoch t, A_t, as the weighted average of the deseasonalised series value at the same instant t and the non-seasonal prediction at the previous epoch, that is,

$$A_t = \alpha(\varepsilon_t - S_{t-s}) + (1 - \alpha)(A_{t-1} + B_{t-1}), \quad (11)$$

where α is a constant, named smoothing parameter, with values in the interval $[0, 1]$.

With the equation

$$B_t = \beta(A_t - A_{t-1}) + (1 - \beta)B_{t-1}, \quad (12)$$

the slope can be estimated as the weighted average of the slope at the previous epoch and its corresponding level change. The smoothing parameter β can have values in the interval $[0, 1]$.

The last equation determines the seasonal component at epoch t, S_t, as the weighted average of the detrended series and the seasonal value at the equivalent epoch in the previous period,

$$S_t = \gamma(\varepsilon_t - A_t) + (1 - \gamma)S_{t-s}, \quad (13)$$

where γ is another smoothing parameter which can also have values in the interval $[0, 1]$.

The smoothing parameters α, β and γ are decisive in the estimation process. Parameter α controls the smoothing of the level equation, so that low values give more importance to historical data, whereas high values weight recent observations. Parameter β modifies the slope estimation in such a way that a value close to 0 gives more importance to trend, whereas a value near 1 weights level changes. Finally, γ controls the smoothing of the seasonal component, so that high values lead to predictions more sensitive to the series variations.

Algorithm 1 implements the Holt–Winters method; its inputs are the number of data per revolution, s, the number of revolutions for which precise observations are available, c, the epoch number, starting after the last available precise observation, for which the series value has to be predicted, h, and the error series $\{\varepsilon_t\}_{t=1}^{T}$ values with $T = s \times c$. The algorithm is designed to produce $\hat{\varepsilon}_{T+h|T}$ as the output, which represents the time-series forecast at the final instant

$t_f = T + h$, based on the time-series value at the end of the control period T.

Algorithm 1. Holt–Winters

Require s, c, h and $\{\varepsilon_t\}_{t=1}^{T}$
Ensure $\hat{\varepsilon}_{T+h|T}$
1: Estimate the values of $A_0, B_0, S_{-s+1}, \ldots, S_{-1}, S_0$
2: **for** $t = 1; t \leqslant T; t = t + 1$ **do**
3: $A_t = \alpha(\varepsilon_t - S_{t-s}) + (1-\alpha)(A_{t-1} + B_{t-1})$
4: $B_t = \beta(A_t - A_{t-1}) + (1-\beta)B_{t-1}$
5: $S_t = \gamma(\varepsilon_t - A_t) + (1-\gamma)S_{t-s}$
6: $\hat{\varepsilon}_t = A_{t-1} + B_{t-1} + S_{t-s}$
7: **end for**
8: Select `error_measure` $\in$ {MSE,MAE,MAPE} and obtain it as a function of the smoothing parameters
9: Obtain the smoothing parameters that minimise `error_measure` using the L-BFGS-B method
10: Calculate $A_T, B_T, S_{T-s+1}, \ldots, S_{T-1}, S_T$ for the optimal smoothing parameters
11: $\hat{\varepsilon}_{T+h|T} = A_T + hB_T + S_{T-s+1+h \bmod s}$
12: **return** $\hat{\varepsilon}_{T+h|T}$

The first step consists in estimating the initial values $A_0, B_0, S_{-s+1}, \ldots, S_{-1}$ and S_0 by means of a heuristic method in which, in the first place, a classical additive decomposition into trend and seasonal variation over the two first revolutions of the satellite is performed. By doing so, the initial values of the seasonal component, $S_{-s+1}, \ldots, S_{-1}$ and S_0, are obtained, whereas the linear regression coefficients over the trend lead to the initial values of level and slope, A_0 and B_0. Once these values have been obtained, the next step can be undertaken, in order to apply the recursive equations which allow for the calculation of the values of the components A_t, B_t and S_t, as well as the single-step error prediction $\hat{\varepsilon}_t$ for control data, i.e. for $t = 1, \ldots, T$ (lines 2–7). These values will remain as functions of the smoothing parameters α, β and γ. In the next step, one of the error functions is selected

$$\begin{aligned} \mathrm{MSE} &= \frac{1}{T}\sum_{i=1}^{T}(\varepsilon_t - \hat{\varepsilon}_t)^2, \\ \mathrm{MAE} &= \frac{1}{T}\sum_{i=1}^{T}|\varepsilon_t - \hat{\varepsilon}_t|, \\ \mathrm{MAPE} &= \frac{1}{T}\sum_{i=1}^{T}\left|\frac{\varepsilon_t - \hat{\varepsilon}_t}{\varepsilon_t}\right| 100 \end{aligned} \tag{14}$$

and its value is determined as a function of the smoothing parameters. Next, the values of the smoothing parameters that minimise the chosen error function have to be determined. As it is not easy to minimise the error functions (14) analytically, a numerical optimisation method is necessary. The limited memory algorithm L-BFGS-B, which is one of the most usual ones, has been chosen for that purpose. The L-BFGS-B method (Byrd et al., 1995), which is a variation of the BFGS method (Broyden, 1970; Fletcher, 1970; Goldfarb, 1970; Shanno, 1970), named after its creators Broyden, Fletcher, Goldfarb and Shanno, is a quasi-Newton limited memory algorithm that allows optimisation with restrictions, thus permitting to impose limitations on smoothing parameters.

With the optimal smoothing parameters, the level and slope values for the last control data (A_T and B_T) are calculated, as well as the seasonal component values for the last revolution in control data ($S_{T-s+1}, \ldots, S_{T-1}, S_T$). With these data, it is possible to predict the value of the series h epochs ahead, $\hat{\varepsilon}_{T+h|T}$ (line 11).

5. Validation of the methodology

The proposed methodology is applied to the *main problem* of the artificial satellite theory so as to model the effect produced by the flattening of the Earth, which corresponds to the J_2 term of Earth's gravitational potential. Three analytical orbit propagator programs (AOPP) are used to conduct this study. They are derived from a second-order closed-form analytical theory based on Lie transforms, which has been briefly described in Section 3. The first AOPP is PPD0, a propagator derived from the zero-order analytical theory, in which only the part corresponding to Kepler's problem has been taken into account. PPD1 is the second propagator; it implements the first-order analytical theory, i.e. the first-order J_2 approximation. Finally, PPD2 implements the second-order analytical theory, i.e. the full second-order J_2 approximation. From each of these AOPPs, a hybrid analytical orbit propagator program (HAOPP) has been developed. In these HAOPPs, statistical time series analysis has been applied to forecast the effects not taken into account in their corresponding initial AOPPs.

The propagator HPPD0 will be used to demonstrate the capability of this methodology to model the full J_2 effect. It is worth noting that this perturbation is not included in the initial propagator PPD0 at all. On the other hand, the propagators HPPD1 and HPPD2 will be used to explore the capability of this methodology to model the error introduced by the analytical approximations, $\mathcal{O}(J_2^2)$ and $\mathcal{O}(J_2^3)$ respectively. In this work, the additive Holt–Winters method will be used for forecasting the effects not taken into account in the initial AOPPs.

Finally, in order to compare and contrast the performance of the HAOPPs, several tests with numerically-simulated initial conditions corresponding to LEO orbits will be performed. The error measure to be considered will be the distance error over a prediction horizon of 30 days.

5.1. Data preprocessing

This methodology starts by choosing the set of variables that will be used for modelling purposes in the forecasting part of the hybrid propagator. In this work, Delaunay

variables have been chosen, although other sets of variables can also be used. After that, in order to build the new propagator, two sets of values corresponding to the same satellite are necessary during the control period. The first consists of accurate values, obtained through the numerical integration of the original problem (4) by using a high-order Runge–Kutta method (Dormand and Prince, 1989), which are considered as actual values from precise observations. The second is obtained by applying the initial integrating part of the hybrid propagator; it contains approximate values which do not include, either in whole or in part, the effect that we want to model in the forecasting part. It is worth noting that the control data should include an amount of values which is enough to identify any pattern that we expect the forecasting part to model and reproduce.

Then, subtracting both data sets for each variable the error time series $(\varepsilon_t^l, \varepsilon_t^g, \varepsilon_t^h, \varepsilon_t^L, \varepsilon_t^G, \varepsilon_t^H)$ are obtained. After this operation, the angular-variable time series $\varepsilon_t^l, \varepsilon_t^g$ and ε_t^h may include some outliers that differ from the rest of values in a quantity multiple of 2π. Such differences correspond to complete spins and, although they have no effect on trigonometrical calculations, for time series analysis they represent abrupt discontinuities in values that are actually very close. Next, by adding or subtracting complete spins (2π), their values can be homogenised to the interval $(-\pi, \pi]$, thus avoiding this and other problems related to the periodic behaviour of these series.

The time series ε_t^H is always 0 for the problem considered here, which means that the pure analytical theory is able to determine H values accurately. Therefore, forecasting of this time series is not necessary. For each of the remaining time series, an univariate Holt–Winters model will be developed from a preliminary analysis so as to forecast its future values. This analysis includes the study of the sequence graphics, periodograms and autocorrelation functions (ACF). These graphics can help reveal the most important characteristics of the series, such as trend, stationarity, atypical values, etc.

Table 1 shows the orbital elements for nine fictitious satellites used for testing the HAOPPs. These initial conditions correspond to LEO orbits and all of them have been chosen to avoid the intrinsic singularities present in Delaunay variables.

Table 1
Satellites used for validation studies of hybrid methodology.

Id	a (km)	e	Inclination (deg)	Period (min)
1	7228	0.0631	49	101.926
2	7876	0.1380	144	115.936
3	7612	0.1132	102	110.156
4	7674	0.1124	68	111.505
5	7064	0.0323	62	98.477
6	7087	0.0504	73	98.959
7	6992	0.0268	29	96.975
8	7269	0.0713	66	102.795
9	7128	0.0499	66	99.819

5.2. Modelling the full J_2 effect

Satellite 1 will be used in this subsection to illustrate this methodology. It is necessary to start mentioning that in the case of the Kepler problem, the orbital elements are constant over time (with the unique exception of the mean anomaly M, which varies between 0 and 2π during each revolution of the satellite). However, adding the J_2 effect to the Kepler problem, i.e. the main problem, produces significant effects on the orbital elements, which include secular, long and short period variations.

Table 2 shows the distance error between PPD0 and the numerical integration of the main problem at different instants. The distance error grows up to a maximum value of about 14,500 km, which represents approximately the distance between perigee and apogee. These values will be used to evaluate the improvement introduced by the hybrid propagators.

The first step in the preliminary analysis consists in plotting the time series $\varepsilon_t^l, \varepsilon_t^g, \varepsilon_t^h, \varepsilon_t^L$ and ε_t^G. Initially, values have been generated every 10 min. Figs. 2 and 3 only show the sequence plots, periodograms and autocorrelation functions of the series $\varepsilon_t^l, \varepsilon_t^h$ and ε_t^L, because the behaviour of ε_t^g and ε_t^G is approximately the same as ε_t^l and ε_t^L respectively.

First, we begin analysing the sequence plots. The series ε_t^l has a linear increasing trend and a periodic behaviour with a period of approximately 33.33 min. On the other hand, the trend of ε_t^h is linear and decreasing, but its periodic behaviour is difficult to discover because it is hidden by its trend, so other statistical tools are needed for its detection. Finally, the trend of ε_t^L is not significant, so it can be considered constant; however, this series shows seasonal fluctuations, the first with a period of almost 50 min, whereas a repetitive pattern of alternate oscillations can be clearly observed approximately every 100 min.

Then, the periodograms and the autocorrelation functions are analysed. It is worth noting that these functions can only be applied to stationary series so, in the first place, it will be necessary to differentiate the series ε_t^l and ε_t^h so as to remove their trends.

The periodogram of $\nabla\varepsilon_t^l$ (Fig. 3) shows that the most significant frequency is close to 0.6π, that is, a periodic behaviour with an approximate period of 33.33 min, whereas series $\nabla\varepsilon_t^h$ and ε_t^L have their main frequency near 0.4π, which corresponds to a period of almost 50 min.

Table 2
Maximum distance error between PPD0 and the numerical integration of the main problem for satellite 1 over different propagation spans.

Time	Distance error (km)
17 h	864.80
1 day	1202.24
2 days	2408.31
7 days	7894.81
30 days	14506.50

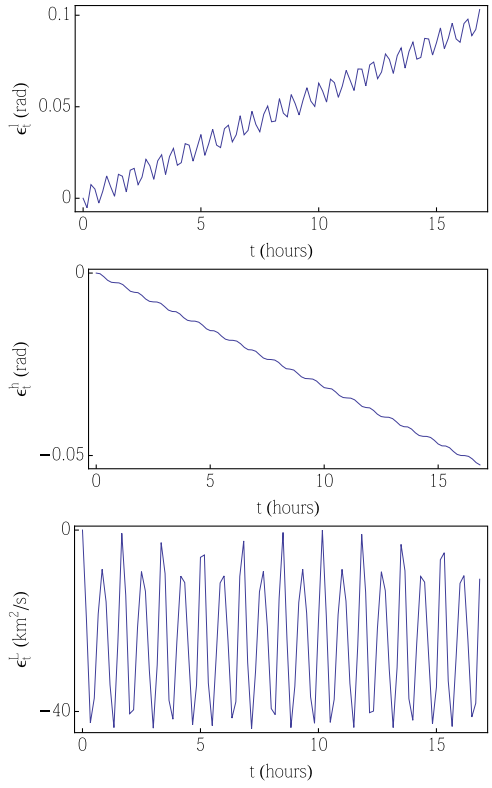

Fig. 2. Sequence plots of the series $\varepsilon_t^l, \varepsilon_t^h$ and ε_t^L.

Finally, from the analysis of the autocorrelation functions of series $\nabla\varepsilon_t^l, \nabla\varepsilon_t^h$ and ε_t^L, it can be observed that, despite having high correlation in several delays, the strongest one corresponds to lag 10, which implies a close relationship each 10 points (approximately each 100 min).

This preliminary analysis allows us to conclude that, although, in principle, it might seem that there are three main periodicities of approximate periods 33.33, 50 and 100 min, in reality, the most remarkable is the last one, which corresponds approximately to the Keplerian period of satellite 1, 101.926 min.

Then, after estimating the initial values A_0, B_0, $S_{-s+1}, \ldots, S_{-s}$ and S_0 by means of the heuristic method described in Section 4, the next step consists in the identification of the optimal values for the smoothing parameters α, β and γ of the Holt–Winters method that minimise the distance error. As shown in Algorithm 1, their values are obtained by applying the L-BFGS-B algorithm to one of the error functions (14), MSE in this case.

Finally, this model is analysed in order to experimentally determine the best amount of control data by choosing the number of both satellite revolutions and points per revolution which minimise the distance error over 30 days,

Table 3
Maximum distance error between HPPD0 and the numerical integration of the main problem for satellite 1 over different propagation spans.

Time	Distance error (km)
17 h	2.69
1 day	2.85
2 days	3.10
7 days	10.83
30 days	13.79

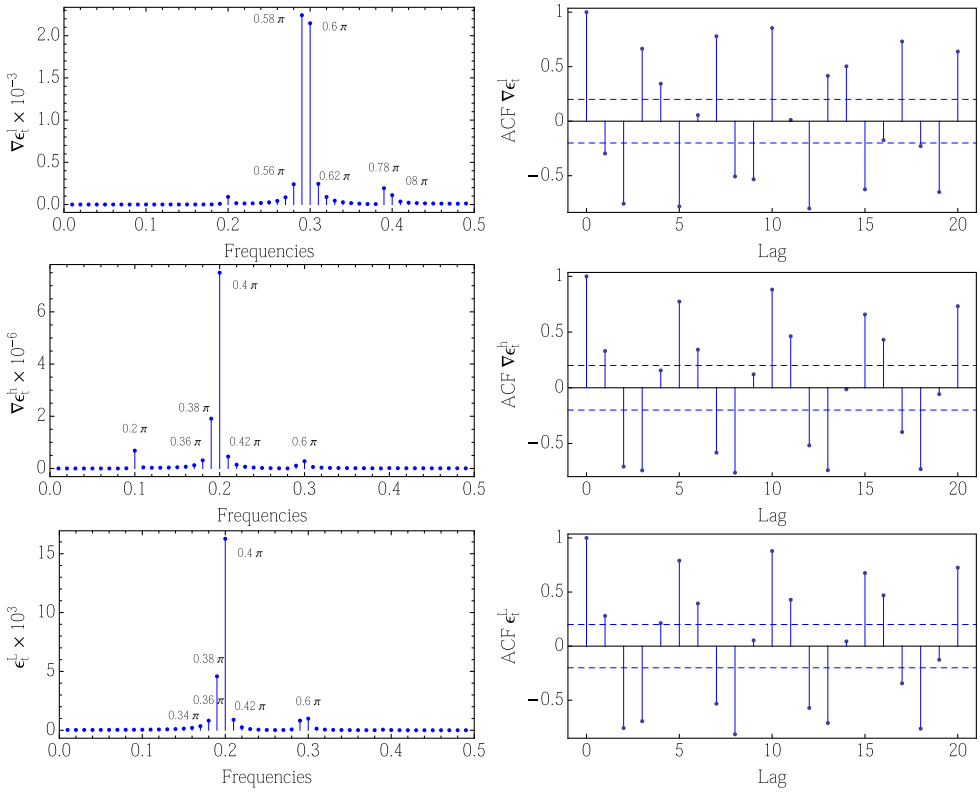

Fig. 3. Periodograms (left) and autocorrelation functions (right) of the series $\varepsilon_t^l, \varepsilon_t^h$ and ε_t^L.

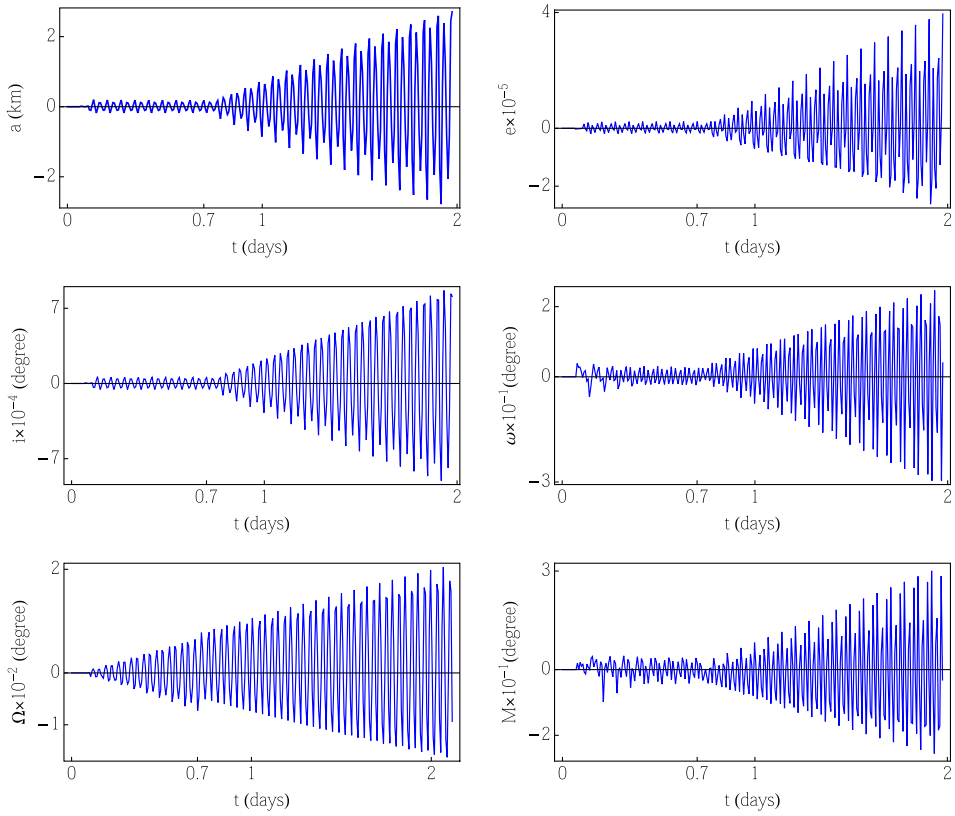

Fig. 4. Evolution of the orbital-element differences between HPPD0 and the numerical integration of the main problem for satellite 1.

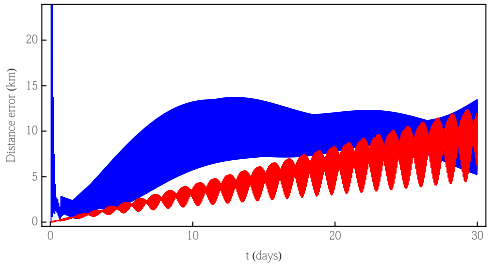

Fig. 5. Distance error of the zero-order hybrid propagator HPPD0 (blue line) and the first-order pure analytical propagator PPD1 (red line) for satellite 1. (For interpretation of the references to colour in this figure caption, the reader is referred to the web version of this article.)

taking into account that we are considering here the Keplerian period as the revolution period. We proceed by fixing the number of revolutions in the first place, with the aim of determining the optimal amount of points per revolution. Once it has been done, the best number of revolutions can be determined. Several configurations have been tested, keeping in mind as general guidelines that the control period has to be long enough so as to contain any dynamics to be modelled, and the sampling rate needs to be high enough so as to capture the highest frequency that the hybrid propagator is designed to model and reproduce. This analysis leads us to consider 10 satellite revolutions and 12 points per revolution as the best choice to constitute the control data for all the studied satellites, which represents a time span of approximately 17 h in the case of satellite 1. More details about this analysis can be found in San-Martín (2014), although further research on this issue is being conducted in order to draw general conclusions regarding the optimal configuration of the control period.

Table 3 shows the distance error between HPPD0 and the numerical integration of the main problem at different instants. As can be seen, the distance error, even after a 30-day propagation, is lower than the pure analytical propagator PPD0 distance error only after 17 h, i.e. the control period.

Fig. 4 shows how the differences between the orbital elements of both HPPD0 and the numerical integration of the main problem evolve during 2 days for satellite 1.

Finally, Fig. 5 compares the distance error for both the zero-order hybrid propagator HPPD0 and the first-order pure analytical propagator PPD1. The error is lower for the analytical propagator during the first 25 days, as could be expected from a higher-order approximation, although both errors become similar as the last part of the 30-day studied period is reached.

5.3. Improving the analytical approximation

In this subsection we study the hybrid propagators based on the first-order and second-order analytical propagators, PPD1 and PPD2 respectively. All the analysed

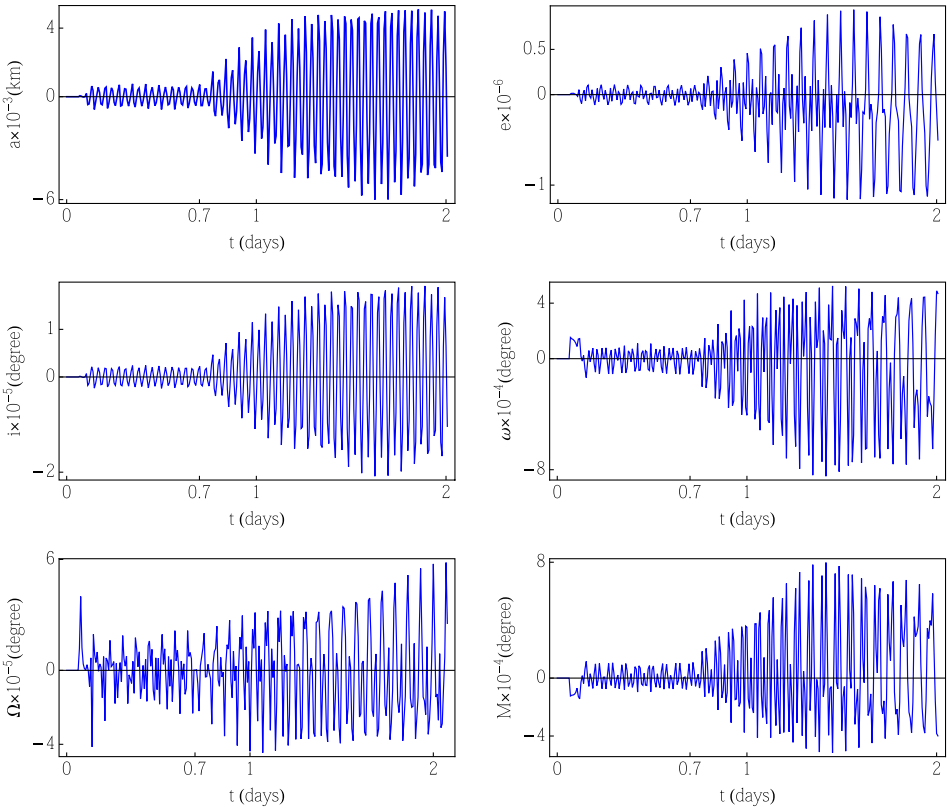

Fig. 6. Evolution of the orbital-element differences between HPPD1 and the numerical integration of the main problem for satellite 1.

Table 4
Distance error of the pure analytical and the hybrid propagators for both first and second-order theories (satellite 1).

Time	PPD1 (km)	HPPD1 (km)	PPD2 (km)	HPPD2 (km)
17 h	0.2758	0.0008	0.0007	4.5×10^{-6}
1 day	0.4037	0.0015	0.0010	8.1×10^{-6}
2 days	0.8223	0.0061	0.0020	1.9×10^{-5}
7 days	2.9175	0.0548	0.0070	4.2×10^{-5}
30 days	12.5706	0.6462	0.0290	4.2×10^{-4}

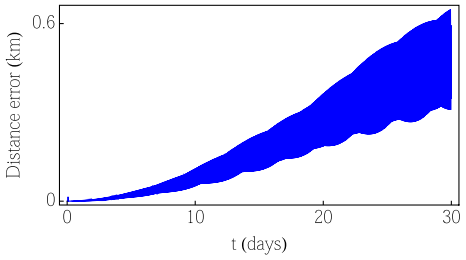

Fig. 7. Distance error of the first-order hybrid propagator HPPD1 for satellite 1.

hybrid propagators improve the accuracy of the analytical theory they are based on; nevertheless, preliminary analysis leads us to conclude that, similarly to the zero-order propagator, optimum results are achieved when the exact revolution period is taken into account, in such a way that the data sampling rate is chosen in order to allow for a complete number of samples per satellite revolution.

Furthermore, the fact that not only periodograms and autocorrelation functions, but also the smoothing parameters to be obtained, are quite similar for the three studied orders of approximation, indicates that the error series $\varepsilon_t^l, \varepsilon_t^g, \varepsilon_t^h, \varepsilon_t^L$ and ε_t^G maintain the same characteristics to be estimated, albeit with decreasing magnitudes for higher-order models, and consequently must be processed and forecasted by means of similar models.

According to what has been expounded, hybrid propagators that consider *MSE* as the error function to be minimised, and take exactly 12 samples, at a regular rate, for each of the 10 revolutions that constitute the control period, are again the most accurate, leading to the best results for short, medium and long-term estimation.

Fig. 6 plots the differences in the evolution of the orbital elements of both the first-order hybrid propagator HPPD1 and the accurate numerical integration of the main problem for satellite 1.

Table 4 shows the predictive capability of both the analytical and associated optimum hybrid propagators. It is worth noting that, after a 30-day propagation, distance error can be reduced by a factor of 20 in the case of first-order theory, or nearly 70 for second-order theory.

Fig. 7 plots the evolution of the distance error for the first-order hybrid propagator HPPD1 during a 30-day time span. It should be noted that the error remains quite low, just about 10 m, for more than 5 days.

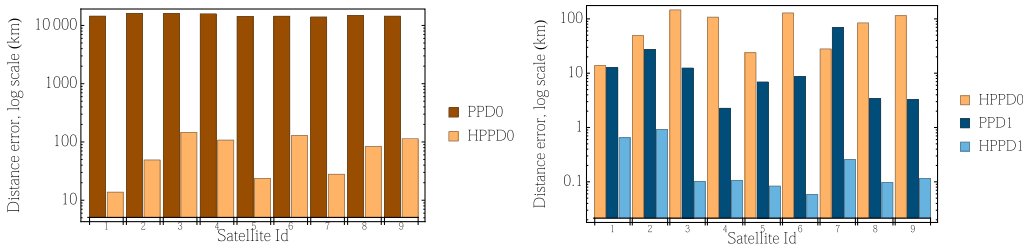

Fig. 8. Distance error of the pure analytical and the hybrid propagators for both zero and first-order theories after a 30-day propagation (satellites 1–9).

Table 5
Distance error of the pure analytical and the hybrid propagators for both zero and first-order theories after a 30-day propagation (satellites 1–9).

Id	PPD0 (km)	HPPD0 (km)	PPD1(km)	HPPD1 (km)
1	14506.5	13.792	12.6	0.634
2	16183.7	49.136	27.3	0.918
3	15987.4	146.465	12.5	0.101
4	15922.4	107.905	2.3	0.106
5	14292.2	23.774	6.9	0.083
6	14456.9	128.633	8.7	0.058
7	14012.8	27.992	68.6	0.255
8	14882.6	84.369	3.4	0.096
9	14489.9	114.199	3.2	0.115

5.4. Hybrid propagators for the complete set of satellites

The importance of acquiring the seasonal variations originated by the satellite revolution period has been verified for satellite 1 in previous subsections. Therefore, for the rest of the satellites, data will also be considered with sampling rates adapted to each satellite period, in such a way that a complete number of samples per revolution is always guaranteed. Apart from that, sequence graphics, periodograms and autocorrelation functions show that, in addition to the revolution-time periodicity, other two periodicities with magnitudes half and third the same satellite revolution time also exist. For those reasons, and with the aim of acquiring such periodic behaviour, it would be desirable to choose a number of samples per revolution which is multiple of both 2 and 3. Taking into account that it is never advisable to consider an amount of data either too high or too low, it is concluded that 12 samples per satellite revolution is an appropriate value as sampling rate also for the remaining 8 satellites.

Fig. 8 and Table 5 show the distance error of the pure analytical and the hybrid propagators for both zero and first-order theories after a 30-day propagation for the complete set of satellites analysed in this work. Taking into account that Fig. 8 has been plotted with logarithmic scale, it should be noted that, in general, the distance error is between 2 and 3 orders of magnitude lower for the hybrid propagator than for the pure analytical propagator in the case of the zero-order theory, i.e. HPPD0 versus PPD0. This hybrid propagator HPPD0 has distance errors between only 0 and 1 orders of magnitude higher than the first-order analytical propagator PPD1, which is one order of approximation higher, although in the case of satellite 7 the hybrid propagator is even more accurate than the superior analytical propagator. When the two first-order propagators are compared, it is found that the hybrid HPPD1 is between 1 and 2 orders of magnitude more accurate than the analytical PPD1.

6. Conclusion

In this work, we have presented a new approach called hybrid perturbation theory. The proposed methodology, which combines an integration method and a prediction technique, has been illustrated through the combination of a simplified general perturbation theory and a statistical time series model based on an additive Holt–Winters method. The hybrid propagators that have been developed have proven an increase in the accuracy of the analytical theory for predicting the position and velocity of the studied orbiters, as well as modelling higher-order terms and other external forces not considered in the analytical theory.

It has been found that the effect of considering a complete number of samples per revolution in hybrid propagators varies depending on the order of the underlying analytical theory, and thus on its margin for improvement. In the case of hybrid propagators based on the zero-order analytical theory, a dramatic reduction in distance error is achieved. In contrast, the second-order hybrid propagator, whose margin for improvement is very reduced, only reaches a slight increase in accuracy when the sample rate is such that a complete number of values fits into a satellite revolution.

Another remarkable conclusion is that similar smoothing parameters are obtained for hybrid propagators based on a certain analytical theory with different orders of approximation, which implies that the error time series to be modelled maintain the same characteristics, even though their magnitude can vary.

Acknowledgments

This work has been funded by the Spanish Finance and Competitiveness Ministry under Project ESP2014–57071-R. The authors would like to thank the reviewers for their valuable suggestions.

References

Aksnes, K., 1970. A second-order artificial satellite theory based on an intermediate orbit. Astron. J. 75, 1066–1076.

Alfriend, K.T., Coffey, S.L., 1984. Elimination of the perigee in the satellite problem. Cel. Mech. 32 (2), 163–172.

Berry, M.M., Healy, L.M., 2004. Implementation of Gauss–Jackson integration for orbit propagation. J. Astronaut. Sci. 52 (3), 331–357.

Brouwer, D., 1959. Solution of the problem of artificial satellite theory without drag. Astron. J. 64, 379–397.

Broyden, C., 1970. The convergence of a class of double-rank minimization algorithms. J. Inst. Math. Appl. 76–79.

Byrd, R.H., Lu, P., Nocedal, J., 1995. A limited memory algorithm for bound constrained optimization. SIAM J. Sci. Stat. Comput. 16 (5), 1190–1208.

Cefola, P.J., Phillion, D., Kim, K.S., 2009. Improving access to the semi-analytical satellite theory. In: AAS/AIAA Astrodynamic Specialist Conference, Pittsburgh, PA, Paper AAS 09-341.

Chan, K., 2010. TSA: time series analysis, R package version 0.98. <http://CRAN.R-project.org/package=TSA>.

Deprit, A., 1969. Canonical transformations depending on a small parameter. Cel. Mech. 1 (1), 12–30.

Deprit, A., 1981. The elimination of the parallax in satellite theory. Cel. Mech. 24, 111–153.

Deprit, A., 1982. Delaunay normalisations. Cel. Mech. 26 (1), 9–21.

Dormand, J.R., Prince, P.J., 1989. Practical Runge–Kutta processes. SIAM J. Sci. Stat. Comput. 10 (5), 977–989.

Fletcher, R., 1970. A new approach to variable metric algorithms. Comput. J., 317–322

Giacaglia, G.E.O., 1964. Notes on von Zeipel's method. Goddard Space Flight Center, Rept. X-547-64-161.

Goldfarb, D., 1970. A family of variable metric updates derived by variational means. Math. Comput., 23–26

Hoots, F.R., France, R.G., 1987. An analytic satellite theory using gravity and a dynamic atmosphere. Cel. Mech. 40 (1), 1–18.

Hoots, F.R., Roehrich, R.L., 1980. Spacetrack report #3: models for propagation of the NORAD element sets. U.S. Air Force Aerospace Defense Command, Colorado Springs, Colorado.

Hori, G.I., 1966. Theory of general perturbations with unspecified canonical variables. Publ. Astron. Soc. Jpn. 18, 287–296.

Hori, G.I., 1971. Theory of general perturbations for non-canonical systems. Publ. Astron. Soc. Jpn. 23, 567–587.

Kinoshita, H., 1977. Third-order solution of an artificial satellite theory. Special Report no. 379, Smithsonian Astrophysical Observatory, Cambridge, Mass, USA.

Kinoshita, H., Nakai, H., 1989. Numerical integration methods in dynamical astronomy. Cel. Mech. 45 (1), 231–244.

Kozai, Y., 1962. Second-order solution of artificial satellite theory without air drag. Astron. J. 67, 446–461.

Krylov, N., Bogoliubov, N.N., 1947. Introduction to Nonlinear Mechanics. Princeton University Press, Princeton, New York.

Liu, J.J.F., Alford, R.L., 1980. Semianalytic theory for a close-Earth artificial satellite. J. Guid. Control Dyn. 3 (4), 304–311.

Long, A.C., Cappellari, J.O., Velez, C.E., Fuchs, A.J., 1989. Goddard trajectory determination system (GTDS) mathematical theory revision 1, CSC/TR-89/6001.

Lyddane, R.N., 1963. Small eccentricities or inclinations in Brouwer theory of the artificial satellite. Astron. J. 68, 555–558.

Morrison, J.A., 1965. Generalized method of averaging and the Von Zeipel method. In: AIAA Astrodynamics Specialist Conference, Monterey, California, Paper AIAA 65-687.

Neelon, J.G., Cefola, P.J., Proulx, R.J., 1997. Current development of the Draper Semianalytical Satellite Theory standalone orbit propagator package. In: AAS/AIAA Astrodynamics Conference, Sun Valley, ID, Paper AAS 97-731.

Pérez, I., San-Juan, J.F., San-Martín, M., López-Ochoa, L.M., 2013. Application of computational intelligence in order to develop hybrid orbit propagation methods. Math. Probl. Eng. 2013 (Article ID 631628), p. 11.

San-Juan, J.F., 1994. ATESAT: automatization of theories and ephemeris in the artificial satellite problem. CNES Technical Report No. CT/TI/MS/MN/94-250.

San-Juan, J.F., 1998. ATESAT: review and improvements. Study of a family of analytical models of the artificial satellite generated by ATESAT and their numerical validation versus PSIMU and MSLIB. CNES Technical Report No. DGA/T/TI/MS/MN/97-258.

San-Juan, J.F., López, L.M., López, R., 2011. MathATESAT: a symbolic-numeric environment in Astrodynamics and Celestial Mechanics. Lect. Notes Comput. Sci. 6783, 436–449.

San-Juan, J.F., San-Martín, M., Pérez, I., 2012. An economic hybrid J_2 analytical orbit propagator program based on SARIMA models. Math. Probl. Eng. 2012 (Article ID 207381), p. 15.

San-Martín, M., 2014. Métodos de propagación híbridos aplicados al problema del satélite artificial. Técnicas de suavizado exponencial (Ph.D. thesis). University of La Rioja, Spain.

Shanno, D., 1970. Conditioning of quasi-Newton methods for function minimization. Math. Comput. 24, 647–656.

Trapletti, A., Hornik, K., 2011. Tseries: time series analysis and computational finance, R package version 0.10-27. <http://CRAN.R-project.org/package=tseries>.

Winters, P.R., 1960. Forecasting sales by exponentially weighted moving averages. Manage. Sci. 6 (3), 324–342.